RSC Advances

ROYAL SOCIETY OF CHEMISTRY

www.rsc.org/advances

Journal Name

ARTICLE

Degradation of atrazine from the riparian zone with the PEC system based on the anode of N-S-TiO_2 nanocrystal-modified TiO_2 nanotubes and the activated carbon photocathode

Received 00th January 20xx,
Accepted 00th January 20xx

DOI: 10.1039/x0xx00000x

www.rsc.org/

Xiongwei Liang[a] , Li Wang[a]*, Fang Ma[a], Huan Lou[b], Xiaofeng Jiang[a], Zhe Li[a]

In this study, we developed a photoelectrochemical (PEC) system based on the anode of N-S-TiO_2 nanocrystal-modified TiO_2 nanotubes and the activated carbon photocathode to degrade atrazine from the riparian zone. This material of N-S-TiO_2/AC was characterized by SEM, XRD, XPS, EDX and fluorescence detection. The characterization results indicated that the systems of NS-TiO_2-TiO_2/AC and NS-TiO_2 NCs/TNTAs–AC/PTFE allowed the highest yield of •OH. According to the simulation results of the absorbance of N-S-TiO_2 with MS, N-S-TiO_2 has the maximum absorbance at 155 nm and 237 nm in the UV region; the average absorbance of N-S-TiO_2 in the visible region was 10000 higher than that of TiO_2. At pH 5.9, N-S-TiO_2 NCs/TiO_2 NTs-AC/PTFE realized the highest atrazine removal rate. Reach 93.89% atrazine removal rate within 150 min in treating water from riparian buffer zone. The PEC system comprising the anode of N-S-TiO_2 nanocrystal-modified TiO_2 nanotubes and the activated carbon photocathode might be an efficient way to remove atrazine in the riparian buffer zone.

Introduction

6-Chloro-*N*^{2}-ethyl-*N*^{4}-isopropyl-1,3,5-triazine-2,4-diamine(atrazine) is one of the most diffusely used herbicides in the world[1]. Although the use of atrazine is banned or regulated in many countries, due to its significant effect on weed control, atrazine is still used in several countries, such as China and Thailand. Atrazine is one of environmental endocrine-disrupting chemicals[2]. Atrazine of 100 ng/L $^{-1}$ to 1 μg/L^{-1} was recorded in surface waters sampled across the world and its degradation period was related to the surrounding environment[3, 4]. Riparian buffer is considered to be one of the most effective methods for the removal of atrazine in non-point source pollution. However, the riparian buffer zone is inefficient in the removal of atrazine[5].

It is feasible to rapidly degrade atrazine in water via the photocatalytic process involving TiO_2[6-8]. The TiO_2 electrode can crack water[9]. TiO_2 is the most widely used photocatalyst in the degradation of organic pollutants from air and water[10]. The PEC system based on the TiO_2 nanomaterial is recognized as one of the most promising methods for the elimination of pollutants, air purification, water decomposition, and solar energy conversion[11-13]. However, the PC efficiency and practical application of TiO_2 nanomaterials are restricted by its intrinsic drawbacks[11, 14-16].

In order to enhance the effect of TiO_2 in the sunlight, great efforts have been carried out. As the band gap semiconductor, bare TiO_2 can be excited only by UV light, which accounts for 5% of the solar spectrum[17, 18]. Moreover, it is difficult to separate and recycle TiO_2 powder in the suspension system[19]. Asahi et al[20] indicated that the PC activity of TiO_2 could be significantly improved when it was doped with N. The N doping can induce the higher energy level (N2p) above the valence band and decrease the required activation energy, thus decreasing TiO_2 band gap in the visible region, improving the absorption capacity, and enhancing the PC efficiency in the visible region. A lot of nonmetallic and metallic elements have been studied to improve the photoresponse (PR) and the PC activity of TiO_2, Related nonmetals included N, C, F, B, and S[21-24] and relevant metals included Fe, Cu, and Cd[25, 26]. NS co-doping is considered to be a more effective way[27].

Although the doped TiO_2 semiconductor is the most commonly used photocatalyst because it is highly stable, non-toxic, and cheap, related studies are focused on the synthesis of light catalysis materials in order to overcome its drawbacks. TiO_2 doped with two or three elements simultaneously has attracted considerable interest because it can induce a higher PR and PC activity[27-30].

Recently, a new highly ordered nanostructure such as nanowires (NWs), nanorods (NRs), nano flakes (NFs), and nanotubes (NTs) were considered to be potential materials due to the strong light harvesting properties and low carrier recombination velocity in PC applications[6, 28, 31, 32]. In these studies, TiO_2 nanotubular has been considered as an ideal nanostructure to improve PC activity. However, the way to overcome the separation efficiency of photo-induced charge carriers is not available, thus limiting its practical application.

[a] State Key Laboratory of Urban Water Resource and Environment, Harbin Institute of Technology, Harbin 150090, China
[b] College of physics and electronic engineering, Henan Normal University, Xinxiang 453007, China
*Corresponding author: Li Wang
Email: Wanglihit@hotmail.com

Electronic Supplementary Information (ESI) available: [details of any supplementary information available should be included here]. See DOI: 10.1039/x0xx00000x

The external potential can promote the transfer of electrons, thus improving the efficiency of the separation of photo generated carriers and PC performance[33-35]. However, the selection of electrode is important for the application of the PEC system. At present, carbon-based materials have showed the wide development prospects due to its special high carrier mobility, mechanical flexibility, optical transparency and chemical stability[36]. Based on the above analysis results, in the established PEC system, the TiO_2 nanotubes modified with N- and S-modified TiO_2 nanocrystals are used as the anode and the activated carbon is used as the PEC cathode. In the PEC system, TiO_2 unitizes visible light and the combination of TiO_2 and activated carbon can accelerate electron transfer, thus improving the PC efficiency. Activate carbon, as a good adsorption material, can adsorb external pollutants, especially atrazine, which is an environmental hormone. Therefore, the atrazine concentration around NS-TiO_2 NCs/TiO_2 NTs is increased, and the PEC system can degrade atrazine more efficiently. It might be used to remove atrazine from the riparian buffer zone.

Experimental

Materials

6-Chloro-N_2-ethyl-N_4-isopropyl-1,3,5-triazine-2,4-diamine(atrazine), tetrabutyl titanate ($TiO(Bu)_4$), hydrofluoric acid (HF), absolute ethanol (EtOH), nitric acid (HNO_3), and thiourea ($CS(NH_2)_2$) were purchased from Sinopharm Chemical Reagent Co., Ltd. All reagents used in this study were of analytical grade and employed without further purification, and distilled (DI) water was used throughout the experiments. The concentration of atrazine from the riparian zone is 0.031mg/L, the concentration of TP and TN respectively for 0.169mg/L and 0.724mg/L, the riparian zone is on the bank of Ashe River which located in Heilongjiang Province, northeast of China.

Construction of the N-S-TiO2 NCs/TNTAs photoelectrode

Typically, highly ordered TiO_2 nano-tube array (TNTAs) were in situ grown through anodization in a two-electrode configuration with as-treated Ti foil anode and Pt foil cathode. Prior to anodization, Ti foils were respectively ultrasonically degreased with acetone, ethanol, and DI water for 10 min, and dried at room temperature (RT). Subsequently, the cleaned Ti foils were immersed in the mixture of HF and diluted HNO_3 acid (HF: HNO_3: H_2O = 1:4:5 in volume) for 30 s, followed by rinsing with DI water. As-cleaned Ti foil was anodized at 20 V for 2 h in the solution containing 0.5 wt% NH_4F and then in glycerol containing 40% (v/v) of DI water. Then, the samples were rinsed with DI water and dried in air. Afterwards, the as-anodized TiO_2 nano-tube arrays were dried at 70 °C for 4 h.
Subsequently, a yellowish Ti_4^+ precursor sol was prepared in accordance with previous studies[20–22]. Typically, a mixture consisting of 10 mL absolute EtOH, 12 mL diluted HNO_3 (1:5, volume ratio of HNO_3 and DI water) and the desired amount of thiourea was added dropwise into another solution containing 40 mL of absolute EtOH and 10 mL $Ti(OBu)_4$ under vigorous stirring. Typically, N- and S-doped TiO_2 NCs-decorated TNTAs (denoted as N-S-TiO_2 NCs/TNTAs) photoelectrodes were prepared through the evaporation-induced self-assembly (EISA) strategy[23]. After it was stirred for 120 min, the as-prepared amorphous TiO_2 nano-tube arrays were immersed into the as-prepared yellowish Ti_4^+ precursor sol for 30 min, followed closely by rinsing with DI water. The above EISA steps were replicated three times. Finally, the decorated TNTAs electrodes were dried at 70 °C for 4 h and then annealed at 500 °C for 2 h. The above method was from the results by Xiuwen Cheng[37].

Typically, highly ordered TiO_2 nano-tube array (TNTAs) were in situ grown through anodization in a two-electrode configuration with as-treated Ti foil anode and Pt foil cathode. Prior to anodization, Ti foils were respectively ultrasonically degreased with acetone, ethanol, and DI water for 10 min, and dried at room temperature (RT). Subsequently, the cleaned Ti foils were immersed in the mixture of HF and diluted HNO_3 acid (HF: HNO_3: H_2O = 1:4:5 in volume) for 30 s, followed by rinsing with DI water. As-cleaned Ti foil was anodized at 20 V for 2 h in the solution containing 0.5 wt% NH_4F and then in glycerol containing 40% (v/v) of DI water. Then, the samples were rinsed with DI water and dried in air. Afterwards, the as-anodized TiO_2 nano-tube arrays were dried at 70 °C for 4 h.
Subsequently, a yellowish Ti_4^+ precursor sol was prepared in accordance with previous studies[20–22]. Typically, a mixture consisting of 10 mL absolute EtOH, 12 mL diluted HNO_3 (1:5, volume ratio of HNO_3 and DI water) and the desired amount of thiourea was added dropwise into another solution containing 40 mL of absolute EtOH and 10 mL $Ti(OBu)_4$ under vigorous stirring. Typically, N- and S-doped TiO_2 NCs-decorated TNTAs (denoted as N-S-TiO_2 NCs/TNTAs) photoelectrodes were prepared through the evaporation-induced self-assembly (EISA) strategy[23]. After it was stirred for 120 min, the as-prepared amorphous TiO_2 nano-tube arrays were immersed into the as-prepared yellowish Ti_4^+ precursor sol for 30 min, followed closely by rinsing with DI water. The above EISA steps were replicated three times. Finally, the decorated TNTAs electrodes were dried at 70 °C for 4 h and then annealed at 500 °C for 2 h. The above method was from the results by Xiuwen Cheng[37].

Modification of activated carbon and preparation of cathode

Activated carbon was soaked in 40% NaOH for 48 h, then washed to the neutral pH with deionized water, and placed in the drying box.
AC/PTFE cathode was prepared by rolling the AC powder and PTFE latex with the stainless steel (60-mesh) as the support material. Firstly, the AC powder was sieved through a 50-mesh sieve. Subsequently, the sieved AC (0.45g) was mixed with 10 wt% of PFTE latex (1.125, 1.5 and 2.25g) under vigorously stirring at 333 K in water bath. Afterwards, to obtain the paste composite, absolute ethanol was added dropwise to disperse the solution. Finally, the dark AC/PTFE composite electrode was successfully obtained by rolling the paste mixture on a MT-10-160 machine (Xiongji Machine Factory, China).

Characterization

The as-prepared TNTAs and N-S-TiO_2 NCs/TNTAs photoelectrodes were characterized with X-ray diffractometer with Cu K radiation (XRD, Rigaku D/Max IIIB), field emission scanning electron microscope (FE-SEM, Quanta 200F), the field emission scanning election microscopy (FESEM, Ultra 55, ZEISS) equipped with an energy dispersive spectrometer (EDS, IE450X-Max80, Oxford) was used to examine the EDS, and X-ray photoelectron spectroscopy (XPS, PHI-5700). In addition, the yields of hydroxyl (·OH) radicals at

the photo-illuminated TNTAs/water interface was detected by the photoluminescence technique (PL, FP-6500). Meanwhile, photoluminescence (PL) spectra of bare TNTAs, NS-TiO_2 NCs/TNTAs–AC/PTFE, and TNTAs–AC/PTFE were also recorded on FP-6500 instrument.

Photoelectrochemical (PECH) measurement

The photoelectrochemical performance of N-S-TiO_2/TiO_2 NTs-AC/PTFE PEC, TiO_2 NTs-AC/PTFE PEC and TiO_2 NTs PC were measured in a traditional standard three-electrode configuration using a PQSTA128N electrochemical workstation with TNTAs electrode as the photoanode.

PC and PEC performances

Atrazine is a widely used herbicide in the field and belongs to the class of organic pesticides and environmental disturbance hormone. It may cause agricultural non-point source pollution in the buffer zone.

PC decomposition of atrazine was carried out in a homemade cylindrical quartz reactor, which contained 0.031 mg/L atrazine water solution (pH 6.7). It should be noted, a 350 Watt xenon lamp and optical density of 100 MW square centimeter as an external light source, which is placed in the 16cm light anode. Prior to irradiation, the TiO_2 nanotube electrode was effective for vertical fixation in the reactor and the magnetic stirring (with an 80 RPM stirring rate) was 30 min, and the adsorption / desorption equilibrium was established in the dark. After that, the xenon lamp is turned on. Samples were collected once every 15 min. The concentration of atrazine was determined by chromatography according to the method by L.J. Xu[38].

Quantum chemical simulation

All calculations are performed in Studio Materials 3.2 with CASTEP module by Accelrys Software Inc. The structures of N-S-TiO_2 and TiO_2 and their absorption spectra were simulated.

Results and discussion

The effect of fabricating parameters on the morphology of TiO_2 NTs photoelectrode (FE-SEM and EDX)

It is well known that key assembling parameters control the morphology of TiO_2 nanotubes. Therefore, the materials of TNTAs and NCs/NTAs N-S-TiO_2 were analyzed by electron microscopy. Fig. 1 shows the FE-SEM images of TNTAs and N-S-TiO_2 NCs/NTAs photoelectrodes. As shown in Fig. 1a, TiO_2 nanotubular structures can be clearly observed and an average diameter and thickness are respectively about 110 nm and 20 nm. In N-S-TiO_2 nanocrystals shown in Fig. 1b, no significant morphological change is observed in the morphology of TiO_2 nanotubes. In addition, numerous N-S-TiO_2 nanocrystals are uniformly deposited on the surface of TiO_2 nanotubes. Scrape down the N-S-TiO_2 for electron microscope observation, as it showed in Fig.1b, the diameter of the N-S-TiO_2 crystal is about 7-10nm.

As shown in Fig.1c, the surface of AC treated with NaOH has a larger gap, indicating the better adsorption performance. AC and PTFE in accordance with the ratio of 5:1 bonding can be seen activated carbon exposed on the outside (Fig. 1d). Oxygen in air would be catalyzed to generate H_2O_2 and ·OH.

The EDX measurement was carried out on the sample, as shown in Figure.1e, the results show that the mass ratio of 13:25 is N/S, and the atomic ratio is 6:13. The proportion of N:S is about 1:2, similar with the expected proportion of doping.

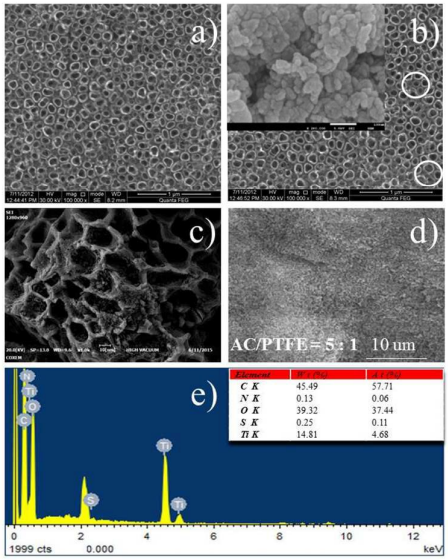

Fig.1. FE-SEM images of TiO_2 NTs (a), N-S-TiO_2 NCs/ TiO_2 NTs (b), active carbon (c), and AC/PTFE electrodes (d) and EDX analysis of N-S-TiO_2 NCs/TiO_2 NTs（e）.

XRD analysis

TiO_2 crystallite plays an important role in PC activity. The XRD patterns of TNTAs and NCs N-S-TiO_2/TNTAs electrodes are shown in Fig.2. Crystal structures of non-doped TiO_2 and N-S-TiO_2 were examined with X-ray diffraction (XRD) and the presence data evidence (JCPDS 1286 - 84) (anatase structure in Fig. 2)[39]. No diffraction peak was observed in the XRD diagram due to the low dopant concentration and the introduction of TiO_2, Ti, and other substances in the gap position of the element. This phenomenon was also observed in previous studies[37, 39]. Unexpectedly, the diffraction peak intensity of the decorated TNTAs was high, indicating that the N- and S-doped TiO_2 nanocrystals were distributed on the surface of TNTAs. The results were consistent with the FE-SEM results. The XRD results showed N and S met the requirements of decorating TNTAs.

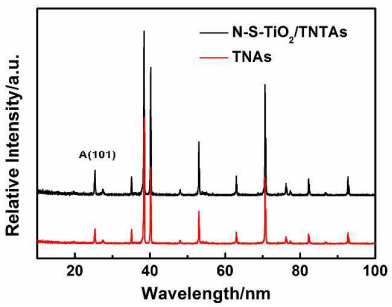

Fig.2. XRD patterns of N-S-TiO_2/TNTAs and TNAs

XPS analysis

In order to study the physical and chemical state of N-S-TiO_2, XPS of the samples were carried out. As it showed in Fig.3. Fig.3a showed the valence state distribution of N in N-S-TiO_2. After fitting the curve, the binding energy in 396.8ev, 399ev and 400.7ev were observed in three distinct peaks. In the 400.7ev peak, the state of N is Ti-O-N or Ti-N, it showed that N replaced TiO_2 in crystal O[40]. At the peak of 396.8ev and 399ev, the N was replaced by N in the state of the anion[20]. This phenomenon shows that N is replaced by O in the TiO_2 crystal, and this phenomenon has been studied in previous studies[27].

Fig.3b showed the valence state distribution of S in N-S-TiO_2, two peaks were observed in the S2p, 167.1 and 170.2 eV respectively, indicating that the S in the TiO_2 doped S^{6+41}, Transformed into S^{4+42}. This phenomenon is related to the preparation environment of N-S-TiO_2[27]. The results show that S and N exist in different valence states in N-S-TiO_2.

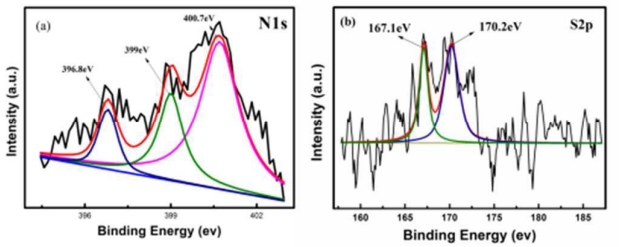

Fig.3. The results of XPS analysis

PECH performence

PECH has been shown to be a powerful technique to study the separation efficiency of photo induced electrons and holes in the PC and PEC reactive interfaces at the TiO_2 electrode. Fig.4 shows the transient photocurrent response (PCR) and open circuit potential (OCP) of the TiO2 NTs-PC, TiO_2 NTs-AC/PTFE-PEC and N-S-TiO_2/TiO_2 NTs-AC/PTFE-PEC, apparently, the photocurrent decreased to zero when the light was turned off, and then transferred to the original value when the lamp was turned on again, indicating that the photocurrent was completely due to the activity of the electrode. As it show in Fig.4, N-S-TiO_2/TiO_2 NTs-AC/PTFE PEC can reach 1.21 mA/cm^2, better than TiO_2 NTs-AC/PTFE PEC（0.96 mA/cm^2）and TiO_2 NTs PC（0.72 mA/cm^2）. This indicates that the N-S-TiO_2/TiO_2 NTs-AC/PTFE PEC can obviously improve the separation efficiency of the photo induced carriers.

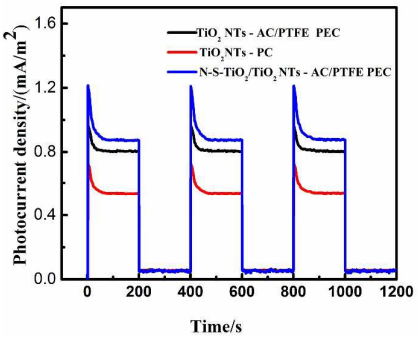

Fig.4. Transient photocurrent response of N-S-TiO_2/TiO_2 NTs–AC/PTFE PEC, TiO_2 NTS-AC/PTFE PEC and TiO_2 NTs-PC.

Analysis of hydroxyl radicals (·OH)

Generally, radical ·OH is considered as the main active substance in the PC reaction[43]. In order to study the PEC or PC activity of NS-TiO_2/TNTAs (anode) – AC/PTFE (cathode), TNTAs (anode) – AC/PTFE (cathode) and TiO_2 NTs samples, the yields of radical ·OH under the light irradiation at the sample/water interface were measured according to the fluorescence derived in the reaction with terephthalic acid (TA). Fig. 5 shows the variations of PL spectra of 0.5 mM TA solution under Xenon lamp illumination at the wavelength of 315 nm with irradiation time in the presence of NS-TiO_2 NCs/TNTAs–AC/PTFE, TNTAs–AC/PTFE, and TiO_2 NTs. The emission peak was observed at 425 nm. Among the three systems, the PEC system of NS-TiO_2 NCs/TNTAs – AC/PTFE allows the highest yield of ·OH, followed by the TNTAs–AC/PTFE and the TiO_2 NTs–PC. Therefore, N-S-TiO_2 NCs/TNTAs–AC/PTFE sample possesses the higher PC activity.

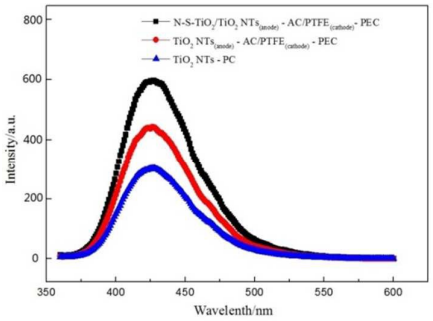

Fig.5. Effects of photoelectrocatalytic systems on fluorescence intensity.

Quantum chemical simulation

MS software was used to simulate the absorption spectra of N-S-TiO_2, as shown in Fig.6. In the cell structure of non-doped TiO_2 shown in Fig.6(a), the gray represents Ti atoms and the red represents O atoms; in the cell structure of N- and S-doped TiO_2 shown in Fig.6(b), the yellow represents S atoms and the blue represents N atoms. The elements N and S were embedded into the TiO_2 crystal lattice. N replaced the position of O atom and S replaced the position of Ti. After the calculation with the MS software, the absorption spectra were obtained (Fig. 7). According to the simulation data, in the ultraviolet region (<380 nm), N-S-TiO_2 showed two peaks at 155 nm and 237 nm. The energy of the ultraviolet region accounts for only about 3% of the energy of the whole sunlight wavelength range. Although N-S-TiO_2 absorption values are much higher in the visible region (380 nm-780 nm), the absorption spectra show a downward trend, and the absorbance values are between 7099 and 65431. In the visible region (380 nm-780 nm), the absorbance value of non-doped TiO_2 also show a downward trend and the absorbance value was between 1098 and 7500[44]. N-S doped TiO_2 had the higher PC activity than the non-doped TiO_2 in the visible light. The solar energy of the visible region accounted for nearly 43% of the energy of the whole sunlight wavelength range. In the visible region, the performance of the modified TiO_2 is much better than that of pure TiO_2[20, 45, 46]. In the infrared region, the absorbance value of modified TiO_2 ranged from 0 to 7099 and the absorbance value of pure TiO_2 ranged from 0 to

1098. At 780 nm, the absorbance value of modified TiO_2 is 6.47 times of that of the pure TiO_2.

As shown in Fig.7, in the ultraviolet region, especially at 155 nm and 237 nm, the absorbance values of pure TiO_2 are higher than those of modified TiO_2. Under the ultraviolet light irradiation conditions, the absorbance value of the pure TiO_2 is better than that of N-S-TiO_2. The peak value in the ultraviolet region is close to 150000, which is 4-5 times of that of the visible light region. In the visible and infrared region, the performance of N-S-TiO_2 is better than that of the pure TiO_2.

In the UV region, the wavelengths at 155 nm and 237 nm are recommended for pure TiO_2, especially ,the wavelength at 237 nm. Artificial ultraviolet light irradiation conditions are not available in the riparian buffer zone and the main energy of sunlight is mainly concentrated in the visible region and infrared region. Therefore, the material of N-S-TiO_2 is recommended.

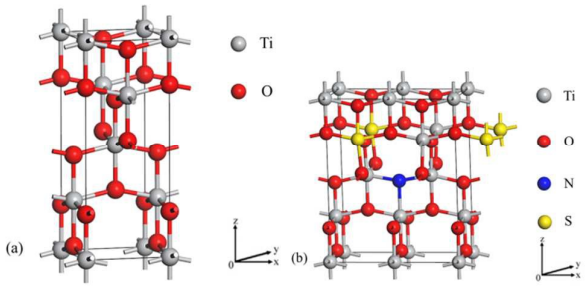

Fig. 6. Cell structures of TiO_2 nanocrystals (a) and N- and S-doped TiO_2 nanocrystals (b).

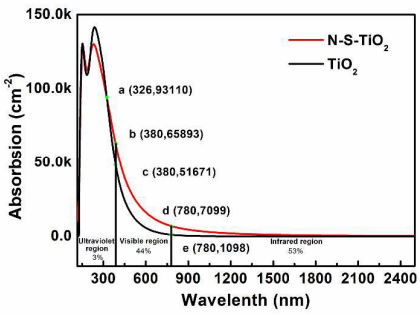

Fig. 7. Absorption spectrum curves of TiO_2 and N-S-TiO_2.

Mechanism of analysis

Usually, hydroxy (·OH) radical was the reactive species during the PC process[47, 48]. Therefore, in order to determine the contribution of each material to the photocatalysis process, we analyzed the mechanism of the PEC system. The generation of radical ·OH radicals has been detected by the fluorescence detection of the reaction with the terephthalic acid (TA) within 30 min[49]. Fig. 3 shows the fluorescence analysis results of TA in three different materials in PEC and PC systems. NS-TiO_2 NCs/TiO_2 NTs was the anode and the AC/PTFE was the cathode, the PEC system of NS-TiO_2/TNTAs (anode) – AC/PTFE (cathode) showed the highest photocatalysis efficiency, followed by the system of TNTAs (anode) – AC/PTFE (cathode) and the TiO_2 NTs photocatalytic system. According to previous studies and the analysis above, we could deduce the mechanism of the PEC system of NS-TiO_2 NCs/TiO_2 NTs - AC/PTFE (Fig. 8). In the photoanode, NS-TiO_2 could absorb and convert more solar energy into chemical energy (Fig.7). The photoelectric chemical reactions in the photoanode are provided as follows:

$$O_2+2H^++2e^-\rightarrow H_2O_2 \quad (3\text{-}1)$$

$$O_2+2H_2O+2e^-\rightarrow H_2O_2+OH^- \quad (3\text{-}2)$$

$$H_2O_2+OH^-\rightarrow H_2O+HO_2^- \quad (3\text{-}3)$$

$$H_2O+HO_2^-\rightarrow \cdot OH+\cdot O_2^-+H_2O \quad (3\text{-}4)$$

Under the influence of sunlight and catalyst, O_2 and H_2O is converted into H_2O_2 ,·OH and $\cdot O_2^-$. According to Eq. (3-5) and Eq. (3-6), it can be inferred that there is a large amount of OH^- accumulated in the photoanode, which limits the PC efficiency[11]. The external voltage can accelerate the transfer of OH^-, which can increase the PC efficiency[50]. In this PEC system, NS-TiO_2 NCs/TiO_2 NTs was the anode and the AC/PTFE was the cathode. N-S-TiO_2 NCs/TNTAs photoelectrodes exhibited intense light absorption in the visible region from 400 nm to 700 nm, high transient PCR of 0.115 $mA\cdot cm^{-2}$, and OCP of −0.312 $mV\cdot cm^{-2}$[37]. The photoelectrodes and cathode could produce a certain voltage, which was conducive to the transfer of OH^-. AC/PTFE could catalyze O_2 into H_2O_2 and ·OH, thus improving the PC performance[6]. In addition, the as-constructed PEC system of N-S-TiO_2 NCs/TiO_2 NTs (photoanode) - AC/PTFE (cathode) exhibited the higher PEC efficiency than that of TiO_2 NTs (photoanode) - AC/PTFE (cathode) system, indicating that AC/PTFE cathode could catalyze oxygen species to form H_2O_2 and ·OH (Fig. 5). At the same time, since activated carbon can adsorb atrazine, the atrazine concentration in the PEC system is increased, thus enhancing PEC efficiency[9].

$$\text{Photoanode}: 4OH^-+4e^-\rightarrow O_2+2H_2O_2 \quad (3\text{-}5)$$

$$\text{Cathode}: 4H_2O+4e^-\rightarrow 2H_2+4OH^- \quad (3\text{-}6)$$

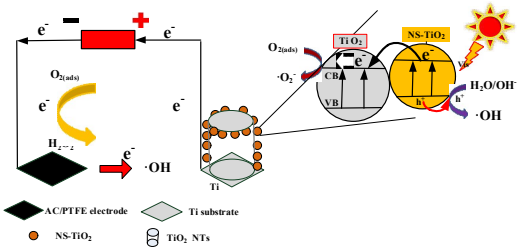

Fig 8. Enhanced PEC performance of the PEC system based on NS-TiO_2 NCs/TiO_2 NTs photoanode and AC/PTFE cathode

Influence of pH

The pH is an important influencing factor of the photocatalytic efficiency of TiO_2 and doped TiO_2[51]. In order to explore the effect of pH on atrazine removal, the pH range of 3.0~9.0 was set in the experiment. The concentration of the NS-TiO_2 NCs/TiO_2 NTs – AC/PTFE was 30 mg/L. The changing trend of atrazine removal rate at different pH values (Fig. 9) showed that the optimal pH was 5.9 and allowed the atrazine removal of 96% after 90-min irradiation. In comparison, the atrazine removal rate was 79% when the pH was 3.0. When the pH increased to 7.0 and 9.0, the removal rate of atrazine decreased to 59% and 65%, respectively. The same trend was previously reported in the degradation of atrazine with photoelectrode, but the degradation effect in the paper was better than previous results[11, 12]. The PEC system might increase the photocatalytic efficiency. It is worth noting that at the pH value of 7

or 9, the surface charge of the catalyst is changed, thus resulting in surface electrostatic exclusion phenomenon and the lower removal rate[52].

The pH in the riparian zone was close to 7[5]. The removal rate of atrazine decreased to 59% after 90 min. Active carbon could absorb atrazine when the surface runoffs brought a large amount of atrazine from cropland. The PEC system could be used to degrade atrazine under the sunshine.

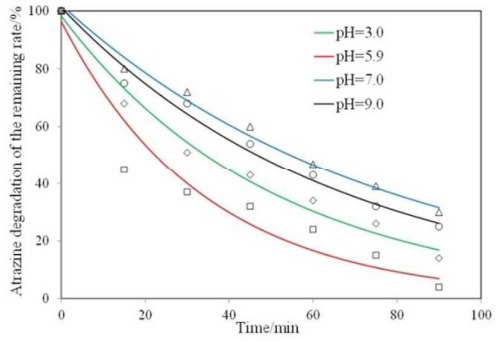

Fig. 9. Atrazine degradation under different pH conditions.

At pH 3.0,5.9,7.0 and 9.0, dry the catalyst before and after reaction, weigh the catalyst, the quality is not reduced, no occurrence of bulging and dregs phenomenon observe the appearance of the catalyst.

Degradation of atrazine from riparian buffer zone (PC and PEC performance)

Water was acquired from the Ashi River riparian buffer. According to testing results, the atrazine concentration was 0.031mg/L and pH was 6.7. After 2-h adsorption, under the simulated sunlight irradiation conditions with neon lamp, we obtained the degradation rate. Fig. 10 shows the degradation rate of atrazine (initial concentration of 0.031 mg/L) in riparian buffer within 150 min at pH 6.7. In the atrazine degradation data of these three materials, N-S-TiO_2/TiO_2 NTs– AC/PTFE shows the fastest atrazine degradation rate, followed by TiO_2 NTs–AC/PTFE and TiO_2 NTs. The degradation rate of atrazine may be related to the concentration of ·OH around atrazine. This can be clearly seen from Figure.3. The degradation rate of atrazine by these three materials showed the same change trend with the concentration of ·OH. In the PEC system of N-S-TiO_2/TiO_2 NTs-AC/PTFE, the declining trend in the first 30 min was more significant than that in the later 20 min because the concentration of atrazine was relatively high at the beginning. After treatment for different periods (30 min, 90 min, 120 min, and 150 min), atrazine degradation rate respectively decreased to 66.13%, 18.12%, 14.12%, and 6.11%. The final atrazine concentration was 0.0019 mg/L and the removal rate obtained in 150 min was 93.89%. The results showed the similar result with the previous results[13].

The removal rate of previous studies was higher due to the use of UV irradiation[53], because under the UV light, the absorption rate of TiO_2 is higher, as shown in Fig.7. Some studies in the 5 h removal rate is about 93%[13]. 20 minutes to get 98.5% of the degradation rate is due to the introduction of microwave in the system[54]. The removal efficiency of *p*-Nitrophenol reached 82.5 % and the COD removal achieved 42.5%[55]. Removal efficiency may be due to the types of external energy, pH, catalyst concentration and removal materials. Compared with the above research, in this paper, the N-S-TiO_2/TiO_2 NTs-AC/PTFE PEC system formed without external energy except sunlight, a closed circuit formed to promote electron transfer, as shown in Figure 8, and N-S doping facilitates the effective absorption of sunlight with the specified region of the conversion and utilization, as shown in Fig. 7. A highly efficient catalytic system was formed. As shown in Fig. 11, the activity of the catalyst was not obviously decreased with five times of reactions, indicating that the catalyst may have a certain future in practical application.

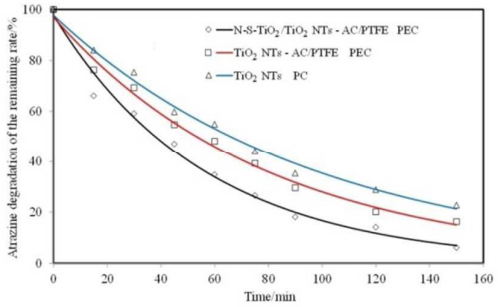

Fig 10. Atrazine degradation of the remaining rate with the three different systems

In the actual riparian buffer zone, the irradiation time is longer[5] and the degradation effect will be better than that of the tested results.

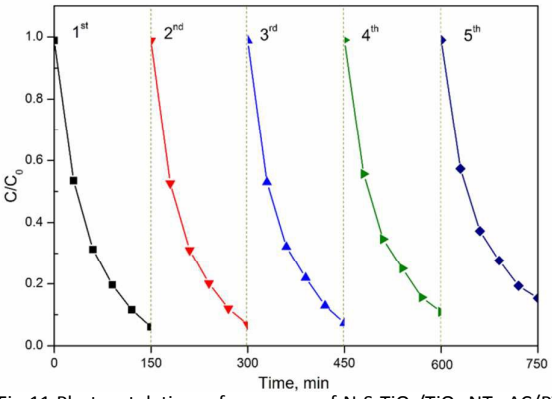

Fig 11.Photocatalytic performences of N-S-TiO_2/TiO_2 NTs AC/PTFE PEC for atrazine dagradation within 5 times uses.

Conclusions

In this study, a PEC system has been used to degrade atrazine from riparian buffer.

According to simulation results, pure TiO_2 at the wavelength of 237 nm showed the highest light absorption performance, indicating that in the ultraviolet region pure TiO_2 should be selected as catalytic materials. However, in the visible region, doped TiO_2 such as N- and S-doped TiO_2, showed the stronger light absorption performance than pure TiO_2, indicating that doped TiO_2 should be selected as catalytic materials in visible region.

Experimental analysis indicated that NS-TiO_2 NCs/TiO_2 NTs could increase the energy absorption of the catalytic material in the

visible region. EC could accelerate the transfer of hydroxyl and electron in the catalytic system.

Activate carbon as EC cathode could adsorb atrazine and increase the concentration of atrazine in the catalytic system, thus improving its catalytic efficiency.

At pH 5.9, NS-TiO_2 NCs/TiO_2 NTs – AC/PTFE showed the best atrazine degradation effect.

After 150-min treatment with the PEC system based on the anode of N-S-TiO_2 nanocrystal-modified TiO_2 nanotubes and the activated carbon photocathode, the degradation atrazine rate from the riparian buffer zone reached 93.89%. The PEC system might be an effective way to degrade atrazine from the riparian buffer in non-point source pollution.

Acknowledgement

This work was supported by National Natural Science Foundation of China (51179041), the Major Science and Technology Program for Water Pollution Control and Treatment (2013ZX07201007), Natural Science Foundation of Heilongjiang Province, China (E201206), Special Fund for Science and Technology Innovation of Harbin (2012RFLXS026), and the State Key Lab of Urban Water Resource and Environment (Harbin Institute of Technology) (No. 2014TS05).

Notes and references

1. D. H. Hutson, *Metabolic Pathways of Agrochemicals: Herbicides and plant growth regulators*, Royal Society of Chemistry, 1998.
2. T. B. Hayes, A. Collins, M. Lee, M. Mendoza, N. Noriega, A. A. Stuart and A. Vonk, *Proceedings of the National Academy of Sciences*, 2002, **99**, 5476-5480.
3. S. P. Schottler and S. J. Eisenreich, *Environmental science & technology*, 1997, **31**, 2616-2625.
4. D. A. Goolsby, E. M. Thurman, M. L. Pomes, M. T. Meyer and W. A. Battaglin, *Environmental science & technology*, 1997, **31**, 1325-1333.
5. R. J. Naiman, H. Decamps and M. E. McClain, *Riparia: ecology, conservation, and management of streamside communities*, Academic Press, 2010.
6. E. Pelizzetti, V. Maurino, C. Minero, V. Carlin, M. L. Tosato, E. Pramauro and O. Zerbinati, *Environmental Science & Technology*, 1990, **24**, 1559-1565.
7. I. Texier, J. Ouazzani, J. Delaire and C. Giannotti, *Tetrahedron*, 1999, **55**, 3401-3412.
8. I. K. Konstantinou, T. M. Sakellarides, V. A. Sakkas and T. A. Albanis, *Environmental Science & Technology*, 2001, **35**, 398-405.
9. B. Li, Z. Lei and Z. Huang, *Chemical Engineering & Technology*, 2009, **32**, 763-770.
10. M. R. Hoffmann, S. T. Martin, W. Choi and D. W. Bahnemann, *Chemical reviews*, 1995, **95**, 69-96.
11. S. Parra, S. Elena Stanca, I. Guasaquillo and K. Ravindranathan Thampi, *Applied Catalysis B: Environmental*, 2004, **51**, 107-116.
12. O. Sacco, V. Vaiano, C. Han, D. Sannino and D. D. Dionysiou, *Applied Catalysis B: Environmental*, 2015, **164**, 462-474.
13. J. Andersen, M. Pelaez, L. Guay, Z. Zhang, K. O'Shea and D. D. Dionysiou, *Journal of Hazardous Materials*, 2013, **260**, 569-575.
14. M. Andersson, L. Österlund, S. Ljungstroem and A. Palmqvist, *The Journal of Physical Chemistry B*, 2002, **106**, 10674-10679.
15. A. Kubacka, M. J. Munoz-Batista, M. Ferrer and M. Fernández-García, *Applied Catalysis B: Environmental*, 2013, **140**, 680-690.
16. M. Bettoni, P. Candori, S. Falcinelli, F. Marmottini, S. Meniconi, C. Rol and G. V. Sebastiani, *Journal of Photochemistry and Photobiology A: Chemistry*, 2013, **268**, 1-6.
17. W. W. Fletcher and R. C. Kirkwood, *Herbicides and plant growth regulators*, Granada Publishing Ltd., 1982.
18. S. K. Joung, T. Amemiya, M. Murabayashi and K. Itoh, *Chemistry-A European Journal*, 2006, **12**, 5526-5534.
19. M. Xing, J. Zhang and F. Chen, *Applied Catalysis B: Environmental*, 2009, **89**, 563-569.
20. R. Asahi, T. Morikawa, T. Ohwaki, K. Aoki and Y. Taga, *science*, 2001, **293**, 269-271.
21. T. Umebayashi, T. Yamaki, H. Itoh and K. Asai, *Applied Physics Letters*, 2002, **81**, 454-456.
22. S. Sakthivel and H. Kisch, *Angewandte Chemie International Edition*, 2003, **42**, 4908-4911.
23. W. Zhao, W. Ma, C. Chen, J. Zhao and Z. Shuai, *Journal of the American Chemical Society*, 2004, **126**, 4782-4783.
24. X. Wang, W. Wang, X. Wang, J. Zhang, J. Zhao, Z. Gu and L. Zhou, *Applied Surface Science*, 2015, **349**, 264-271.
25. J. Choi, H. Park and M. R. Hoffmann, *The Journal of Physical Chemistry C*, 2009, **114**, 783-792.
26. J. Gong, W. Pu, C. Yang and J. Zhang, *Electrochimica Acta*, 2012, **68**, 178-183.
27. X. Cheng, H. Liu, Q. Chen, J. Li and P. Wang, *Electrochimica Acta*, 2013, **103**, 134-142.
28. X. Cheng, X. Yu and Z. Xing, *Journal of colloid and interface science*, 2012, **372**, 1-5.
29. F. Wei, L. Ni and P. Cui, *Journal of Hazardous Materials*, 2008, **156**, 135-140.
30. X. Cheng, X. Yu and Z. Xing, *Materials Research Bulletin*, 2012, **47**, 3804-3809.
31. S. HyukáIm and J. HyeokáPark, *Chemical Communications*, 2010, **46**, 2385-2387.
32. Q. Chen, H. Liu, Y. Xin, X. Cheng and J. Li, *Applied Surface Science*, 2013, **264**, 476-484.
33. H. G. Oliveira, D. C. Nery and C. Longo, *Applied Catalysis B: Environmental*, 2010, **93**, 205-211.
34. V. Jaeger, W. Wilson and V. R. Subramanian, *Applied Catalysis B: Environmental*, 2011, **110**, 6-13.
35. R. Daghrir, P. Drogui and D. Robert, *Journal of Photochemistry and Photobiology A: Chemistry*, 2012, **238**, 41-52.
36. H. Irie, Y. Watanabe and K. Hashimoto, *Chemistry Letters*, 2003, **32**, 772-773.
37. X. Cheng, H. Liu, Q. Chen, J. Li and P. Wang, *Electrochimica Acta*, 2013, **103**, 134-142.
38. L. Xu, W. Chu and N. Graham, *Journal of hazardous materials*, 2014, **275**, 166-174.
39. J. Yu, G. Dai and B. Cheng, *The Journal of Physical Chemistry C*, 2010, **114**, 19378-19385.

40. T. Sano, N. Negishi, K. Koike, K. Takeuchi and S. Matsuzawa, *Journal of Materials Chemistry*, 2004, **14**, 380-384.
41. S. Liu and X. Chen, *Journal of Hazardous Materials*, 2008, **152**, 48-55.
42. M. Zhou and J. Yu, *Journal of Hazardous Materials*, 2008, **152**, 1229-1236.
43. W. Li, D. Li, Y. Lin, P. Wang, W. Chen, X. Fu and Y. Shao, *Journal of Physical Chemistry C*, 2012, **116**, 3552-3560.
44. Z. Zhao and Q. Liu, *Journal of Physics D: Applied Physics*, 2008, **41**, 025105.
45. X. Cheng, X. Yu and Z. Xing, *Applied Surface Science*, 2012, **258**, 3244-3248.
46. X. Chen and S. S. Mao, *Chemical Reviews*, 2007, **107**, 2891-2959.
47. X. Cheng, H. Liu, X. Yu, Q. Chen, J. Li, P. Wang, A. Umar and Q. Wang, *Science of Advanced Materials*, 2013, **5**, 1563-1570.
48. W. Li, D. Li, Y. Lin, P. Wang, W. Chen, X. Fu and Y. Shao, *The Journal of Physical Chemistry C*, 2012, **116**, 3552-3560.
49. K.-i. Ishibashi, A. Fujishima, T. Watanabe and K. Hashimoto, *Electrochemistry Communications*, 2000, **2**, 207-210.
50. X. Cheng, G. Pan and X. Yu, *Chemical Engineering Journal*, 2015, **279**, 264-272.
51. M. M. Islam and S. Basu, *Journal of Environmental Chemical Engineering*, 2015, **3**, 2323-2330.
52. S. Parra, S. E. Stanca, I. Guasaquillo and K. Ravindranathan Thampi, *Applied Catalysis B: Environmental*, 2004, **51**, 107-116.
53. T. A. McMurray, P. S. M. Dunlop and J. A. Byrne, *Journal of Photochemistry and Photobiology A: Chemistry*, 2006, **182**, 43-51.
54. G. Zhanqi, Y. Shaogui, T. Na and S. Cheng, *Journal of Hazardous Materials*, 2007, **145**, 424-430.
55. Z. Hu, M. Zhou, L. Zhou, Y. Li and C. Zhang, *Environmental Science and Pollution Research*, 2014, **21**, 8476-8484.

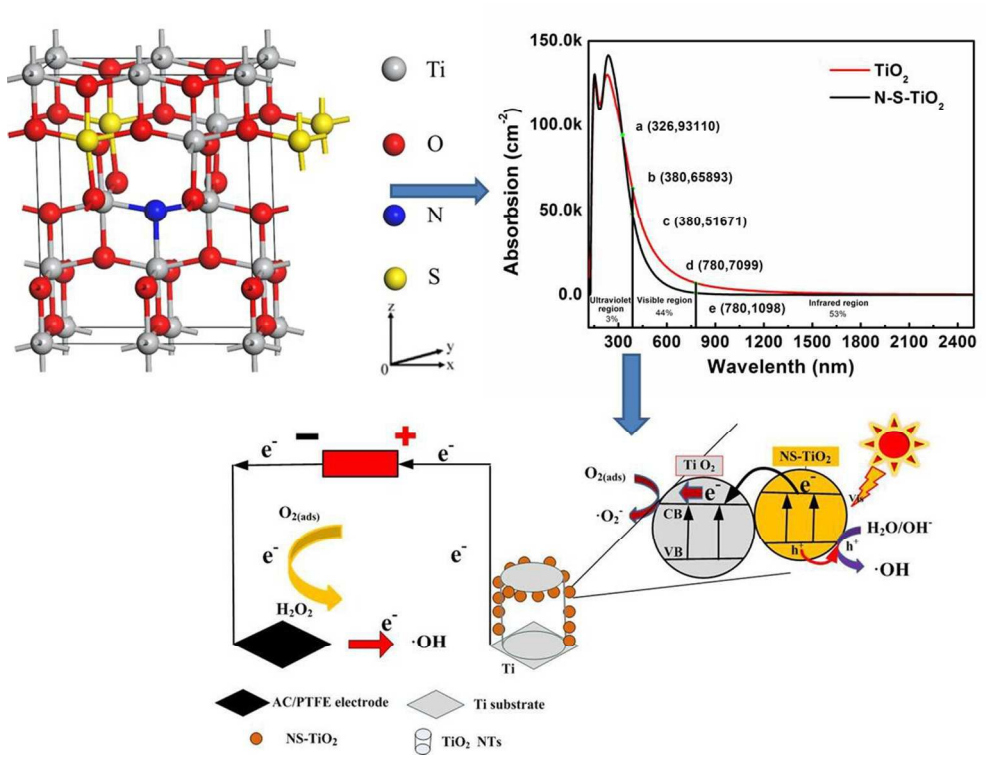

313x234mm (96 x 96 DPI)